

In Vivo Determination of RNA Structure–Function Relationships: Analysis of the 790 Loop in Ribosomal RNA

KangSeok Lee¹, Shikha Varma², John SantaLucia Jr²
and Philip R. Cunningham^{1*}

¹Department of Biological Sciences, Wayne State University, Detroit MI 48202, USA

²Department of Chemistry Wayne State University Detroit, MI 48202, USA

The 790 loop is a conserved hairpin located between positions 786 and 796 of *Escherichia coli* 16S rRNA that is required for ribosome function. Using a novel genetic approach, all positions in the loop were simultaneously mutated and functional mutant sequences were selected *in vivo*. This “instant evolution” experiment revealed that approximately 190 of the 262,144 possible mutant sequences were functional. Analysis of functional mutant sequences allowed discrimination between nucleotides directly involved in protein synthesis and those involved primarily in loop structure. Among the functional mutant sequences, positions 789 and 791 were invariant and extensive covariation was observed among the nucleotides at the base of the loop at positions 787, 788, 794 and 795. NMR and thermodynamic analyses of model 790 hairpins *in vitro* revealed weak pairing interactions between positions 787 and 795 and between positions 788 and 794 consistent with the *in vivo* mutational analysis. Functional analysis of site-directed mutants containing all possible nucleotide combinations at positions 787 and 795 *in vivo* showed that stable base-pairs at these positions prevent subunit association.

© 1997 Academic Press Limited

*Corresponding author

Keywords: 790 loop; ribosomal RNA; instant evolution; NMR; mutation

Introduction

Ribosomal RNA has been functionally implicated in virtually every aspect of protein synthesis (Barta *et al.*, 1984; Cundliffe, 1986; Cunningham *et al.*, 1993; Dahlberg, 1989; de Stasio *et al.*, 1988; Noller, 1991; Noller *et al.*, 1992) and a number of biochemical, physical and genetic approaches have been taken to elucidate the molecular mechanisms involved (Zimmermann & Dahlberg, 1996). An important aspect of ribosomal RNA functional analysis by any method is the ability to distinguish between direct effects on ribosome function and indirect effects attributable to perturbations of rRNA structure (Cunningham *et al.*, 1992, 1993; Fourmy *et al.*, 1996; Huang *et al.*, 1996; Lodmell *et al.*, 1995;

Lu & Draper, 1995; Moine & Dahlberg, 1994; Ryan & Draper, 1991; Szewczak & Moore, 1995).

The 790 loop (positions 786 to 796 in *Escherichia coli* 16S rRNA, Figure 1) is found in the small subunit ribosomal RNAs of all organisms (Gutell, 1994) and has been implicated in subunit association (Herr *et al.*, 1979; Tapprich & Hill, 1986; Tapprich *et al.*, 1989), initiation factor 3 binding (Moazed *et al.*, 1995; Muralikrishna & Wickstrom, 1989; Tapprich *et al.*, 1989) and tRNA binding (Moazed & Noller, 1986). This loop is exposed to solvent in the small subunit and is located at the interface between the large and small subunits in 70S ribosomes (Chapman, 1977; Lata *et al.*, 1996; Santer & Shane, 1977; Tapprich & Hill, 1986). Here, we report the development of a method for “instant evolution” in which random mutagenesis and *in vivo* selection are used to identify both structural and functional features of the 790 loop. Structure predictions based upon the instant evolution approach are confirmed by NMR and thermodynamic analysis of oligonucleotide hairpins.

Abbreviations used: 1D and 2D, one and two-dimensional; NOE, nuclear Overhauser effect; NOESY, NOE spectroscopy; ppm, parts per million; CAT, chloramphenicol acetyltransferase; MIC, minimal inhibitory concentration; MBS, message binding sequence; RBS, rRNA binding sequence.

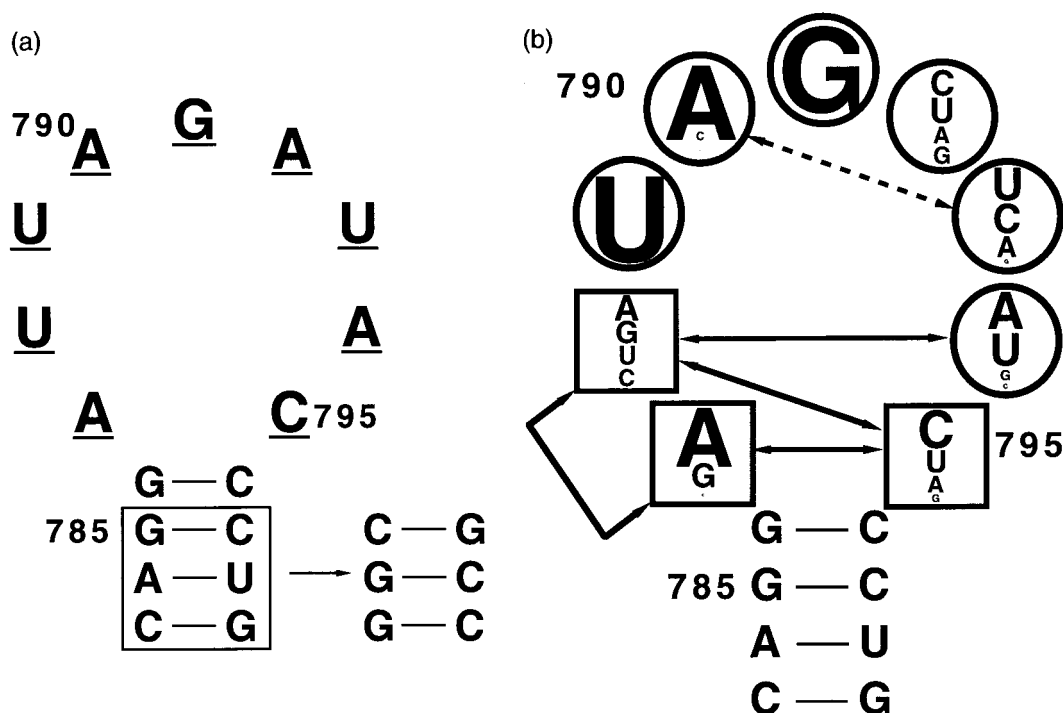


Figure 1. (a) Sequence of *E. coli* 790 hairpin. Nucleotides mutated in this study are underlined. The bottom three base-pairs of the stem (boxed) are not conserved and were substituted as indicated for NMR and thermodynamic studies to minimize fraying artifacts. (b) Analysis of 790 loop mutants. Nucleotide preferences for each mutated position are shown and scaled to reflect the frequencies in Table 2. Nucleotide covariations are indicated by arrows. A broken line denotes the location of a covariation that has not yet been confirmed by physical measurements (see the text). Positions where nucleotide identity significantly correlated with function (MIC) are boxed.

Results and Discussion

Random mutagenesis and selection of functional alternative 790 loop sequences

We recently reported the identification and analysis of a number of alternative functional mutants in the message-binding sequence of rRNA and the ribosome-binding sequence of mRNA (Lee *et al.*, 1996). These data were used to construct a genetic system to study the relationship between structure and function in the 790 loop *in vivo*. In this system, the chloramphenicol acetyltransferase (CAT) reporter message (Burns & Crowl, 1987) is translated exclusively by plasmid-encoded ribosomes that cannot translate normal cellular messages (Hui & De Boer, 1987; Lee *et al.*, 1996: see Figure 2). Consequently, cells containing this construct (pRNA122, Figure 2) are chloramphenicol-resistant and the level of this resistance is directly dependent upon the amount of functional CAT protein produced by the plasmid-derived ribosomes. Thus, deleterious rRNA mutations in plasmid-encoded ribosomes inhibit translation of only the CAT message, resulting in lower chloramphenicol resistance without affecting translation of other cellular messages.

Sequence analysis of functional mutants

Random mutations were introduced simultaneously at all nine positions (787 to 795) in the

790 loop. Functional (chloramphenicol-resistant) mutants were then selected in *E. coli* DH5 cells (Hanahan, 1983) and the effects of these mutations on ribosome function were determined. A total of 182 mutants that retained chloramphenicol resistance were randomly selected and sequenced. Wild-type 790-loop sequences were obtained from 81 of the sequenced transformants, while the remaining 101 contained mutant sequences. One of the transformants was chloramphenicol-resistant in the absence of inducer, presumably due to a spontaneous mutation in the CAT gene, and was excluded from further analysis. Of 100 sequenced functional mutants, 14 were duplicates and four sequences occurred three times. Thus, 78 different, functional, 790-loop mutants were analyzed (Table 1). According to resampling theory, this distribution indicates that of the $4^9 = 262,144$ possible sequences, only 190 (standard deviation 30) unique sequences exist in the pool of selected functional mutants. Of the 78 mutants, 44 contained four to six substitutions out of the nine bases mutated and 21 of these retained greater than 50% of the wild-type activity. The minimal inhibitory concentration (MIC) of chloramphenicol for cells expressing wild-type rRNA from pRNA122 is 600 $\mu\text{g/ml}$. MICs of the mutants ranged from 150 to 550 $\mu\text{g/ml}$ with a mean of 320 $\mu\text{g/ml}$ (standard deviation 89). The median and mode were both 350 $\mu\text{g/ml}$.

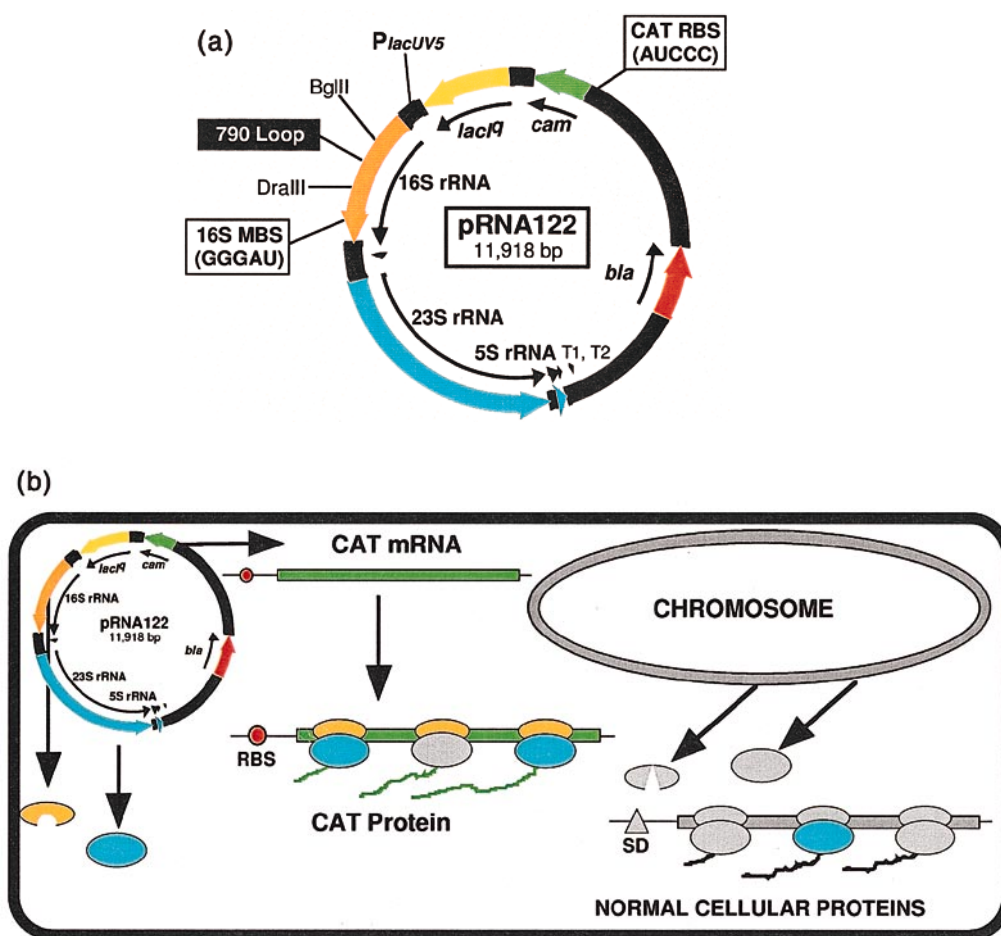


Figure 2. System for genetic analysis of rRNA function. (a) Plasmid map of pRNA122. Transcription of the rRNA operon (*rnmB*) is driven by the inducible *lacUV5* promoter (*PlacUV5*). The *lac* repressor gene (*lacI^q*) allows regulation of *rnmB* transcription. CAT gene (*cam*) transcription is constitutive (Hui *et al.*, 1987). The message binding sequence (MBS) of 16 S rRNA and rRNA binding sequence (RBS) of the CAT message were changed as indicated (boxed) to allow targeting of CAT mRNA specifically to plasmid-encoded ribosomes (Lee *et al.*, 1996). *bla*, ampicillin resistance. *Bgl*II and *Dra*III, restriction sites discussed in the text. T1 and T2, *rnmB* transcriptional terminators. (b) Segregation of plasmid and chromosomal-mediated protein synthesis. Orange ovals, plasmid-encoded 30 S ribosomal subunits. Blue ovals, plasmid-encoded 50 S ribosomal subunits. Gray ovals, chromosome-encoded ribosomes. In the absence of inducer (IPTG), cells carrying pRNA122 are resistant to 40 μ g/ml chloramphenicol (MIC 50 μ g/ml) due to low-level transcription of the *rnmB* operon (data not shown). Induced cells (1 mM IPTG) are resistant to 550 μ g/ml (MIC 600 μ g/ml). SD, Shine-Dalgarno sequence (Shine & Dalgarno, 1974).

Functional 790-loop mutants showed strong nucleotide preferences at all mutated positions, except positions 788 and 792, which showed a random distribution (Table 2) but significant covariation (Figure 1, and see below). No mutations were observed at U789 or G791. Mutations at these positions, however, were present in mutants that were selected for loss of function (not shown). Thus, these nucleotides appear to be directly involved in ribosome function. U789 is strictly conserved among bacteria but is frequently C789 among other organisms (Table 2). Chemical protection studies have shown that G791 is specifically protected from kethoxal modification in 70 S ribosomes and polysomes (Brow & Noller, 1983; Moazed & Noller, 1986) and by poly(U) (Moazed & Noller, 1986) and that G791 becomes more acces-

sible to kethoxal modification when 30 S subunits are converted from the "inactive" to "active" conformation (Moazed *et al.*, 1986).

Purines were strongly selected at position 787 (97.4%) while A and, to a lesser extent, C were preferred at position 790 (98.7%) and U was completely excluded at both positions. At both position 793 and 795, A, C and U were equally distributed but G was selected against. Adenine and uracil were preferred at position 794 (81.8%).

Non-random distribution of nucleotides among the selected functional clones indicates that nucleotide identity affects the level of ribosome function. To examine this, the mean activities (MICs) of ribosomes containing all mutations at a given position were compared by single-factor analysis of variance between ribosome function

Table 1. continued

MIC ^a (µg/ml)	787	788	789	Nucleotide sequence ^b						Number of mutations ^c	Number of occurrences ^d
				790	791	792	793	794	795		
200	A	<u>C</u>	U	A	G	A	<u>G</u>	U	C	3	1
200	A	<u>A</u>	U	<u>C</u>	G	<u>C</u>	<u>A</u>	<u>G</u>	C	5	1
200	<u>C</u>	<u>A</u>	U	A	G	<u>U</u>	U	<u>U</u>	<u>U</u>	5	1
200	<u>G</u>	<u>G</u>	U	A	G	<u>A</u>	U	<u>G</u>	<u>U</u>	4	1
200	<u>G</u>	<u>G</u>	U	A	G	<u>U</u>	C	<u>G</u>	<u>U</u>	6	1
200	<u>G</u>	<u>G</u>	U	<u>C</u>	G	<u>C</u>	U	A	<u>U</u>	5	1
200	<u>G</u>	<u>C</u>	U	<u>A</u>	G	<u>U</u>	<u>A</u>	A	<u>G</u>	5	1
150	<u>G</u>	<u>G</u>	U	A	G	<u>C</u>	U	U	<u>G</u>	5	1

^a Sequences are ranked by the minimum inhibitory concentration (MIC) of chloramphenicol required to fully inhibit growth of cells expressing the mutant ribosomes.

^b The 790 loop sequences selected from the pool of functional, randomized mutants. Mutations are underlined.

^c Number of mutations in each mutant sequence.

^d Number of clones with the indicated sequence.

^e Sequence and activity of the unmutated control, pRNA122. (WT, wild-type).

(MIC) and nucleotide identity at each mutated position. Positions that showed a significant effect of nucleotide identity upon the level of ribosome function were 787 ($P < 0.001$), 788 ($P < 0.05$) and 795 ($P < 0.001$) (Figure 1(b)). The absence of mutations at positions U789 and G791 in the functional clones prevents statistical analysis of these positions but mutations at these positions presumably strongly affect ribosome function as well.

Table 2 shows a comparison of the selected functional mutants with current phylogenetic data (R. Gutell, unpublished results; Gutell, 1994; Maidak *et al.*, 1996). While nucleotide preferences in the se-

lected mutants are similar to those observed in the phylogenetic data, the mutant sequences selected in this study show much more variability than those found in nature. This may be because all of the positions in the loop were mutated simultaneously, allowing normally deleterious mutations in one position to be compensated for by mutations at other positions, a process that is unlikely to occur in nature. In addition, none of the mutants was as functional as the wild-type, suggesting that wild-type 790-loop sequences have been selected for optimal activity or that other portions of the translational machinery have been optimized to function with the wild-type sequence.

Table 2. 790-loop sequence variation

Nucleotide	787	788	789	790	791	792	793	794	795	
A. Nucleotide distribution of functional mutants ^a										
A	<u>54</u>	24	0	<u>69</u>	0	<u>15</u>	18	<u>35</u>	16	
C	2	16	0	8	0	24	26	5	<u>34</u>	
G	22	21	0	1	<u>78</u>	16	4	9	<u>7</u>	
U	0	<u>17</u>	<u>78</u>	0	0	23	<u>30</u>	29	21	
Consensus	R	N	U	M	G	N	H	W	H	
B. Nucleotide distribution in all known bacteria ^b										
A	<u>573</u>	0	0	<u>578</u>	1	<u>578</u>	0	<u>577</u>	0	
C	3	0	0	0	1	0	0	1	<u>578</u>	
G	1	0	0	0	<u>576</u>	0	3	0	0	
U	1	<u>578</u>	<u>578</u>	0	0	0	<u>575</u>	0	0	
Consensus	A	U	U	A	G	A	U	A	C	
C. Nucleotide distribution in all known organisms ^c										
A	<u>1657</u>	2	1	<u>1648</u>	2	<u>1655</u>	5	<u>1664</u>	1	
C	6	1	566	9	1	1	12	1	<u>1665</u>	
G	4	0	0	3	<u>1662</u>	7	46	2	0	
U	1	<u>1664</u>	<u>1101</u>	7	3	3	<u>1605</u>	1	0	
Δ	0	1	0	1	0	2	0	0	2	
Consensus	A	U	Y	A	G	A	U	A	C	

Consensus: R = A or G; N = A, C, G or U; M = A or C; H = A, C or U; W = A or U; Y = C or U. Δ = deletion. Underlined numbers indicate the wild-type *E. coli* sequence.

^a Nucleotide distribution of the 78 functional 790 loop mutants. Mutants containing nucleotide substitutions different from the consensus (C787, G790, G793, C794 and G795) were confirmed by transferring the *Bgl*III-*Dra*III fragment containing the mutations to pRNA122 (Figure 2) and sequenced between ligation junctions. All transformants showed the same level of chloramphenicol resistance as the original isolates, indicating that none of the mutants contained unprogrammed mutations.

^b Phylogenetic variation of 790 loop nucleotides in bacterial ribosomes (Gutell, 1994; R. Gutell, unpublished results).

^c Phylogenetic variation of 790 loop nucleotides in ribosomes from all known organisms (Gutell, 1994; R. Gutell unpublished results).

To identify potential nucleotide covariation within the loop, the paired distribution of selected nucleotides was examined for goodness of fit. The most significant covariations (Figure 1(b)) were observed between positions 787 and 795 ($P < 0.001$) and between positions 790 and 793 ($P < 0.001$). For positions 790 and 793, only eight double mutants were available for analysis; therefore, the covariation observed between these positions should be regarded with caution. Position 788, which showed no nucleotide specificity, did show significant covariation with positions 787 ($P < 0.01$), 794 ($P < 0.01$) and 795 ($P < 0.01$).

Analysis of site-directed mutations constructed at the base of the loop

Functional analysis of mutations at positions 787 and 795

The observed covariations among positions 787, 788 and 795 (Figure 1(b)) are particularly interesting, since nucleotide identity at these positions correlated with the level of ribosome function. Further analysis of nucleotides at positions 787 and 795 revealed that 72 of the 78 functional mutants have the potential to form mismatched base-pairs (A·C, G·U, A·A and G·G). Other mismatches, such as G·A and U·G, however, were not found. In addition, only four sequences with an A·U Watson-Crick pair and no sequences with a U·A, G·C or C·G pair were present, suggesting that strong base-pairs between these positions inhibit ribosome function. We therefore constructed and analyzed

all possible nucleotide combinations at positions 787 and 795 without changing other nucleotides in the 790 loop. Ribosome function of the mutants (Table 3) varied from 84% (A·A) to 1% (C·G) of the wild-type. As predicted by analysis of the pool of functional random mutants, site-directed mutants with G·C, C·G and U·A Watson-Crick pairs between positions 787 and 795 were strongly inhibitory. These data suggest that strong pairing between nucleotides at positions 787 and 795 inhibits ribosome function. In addition, some of the site-directed substitutions at positions 787 and 795 that produced functional ribosomes were largely excluded from the pool of mutants in which all of the loop positions were mutated simultaneously (e.g. CC, CU, UU and UC). The observed nucleotide preferences at positions 787 and 795 in the selected random pool presumably reflect interaction of nucleotides at these positions with other nucleotides in the loop. This is consistent with our findings of extensive covariations among these sites (Figure 1).

Perturbations of the 790 loop have been shown to affect ribosomal subunit association (Herr *et al.*, 1979; Tappich & Hill, 1986; Tappich *et al.*, 1989). We therefore tested several of the 787 to 795 mutants for their ability to form 70 S ribosomes. Ribosomes were isolated from selected mutants and the distribution of mutant ribosomes in both the 70 S and 30 S peaks was determined by primer extension; and see Table 3). These data show that CAT activity correlates with the presence of mutant 30 S subunits in the 70 S ribosome pool. Thus, loss of

Table 3. Functional and thermodynamic analysis of positions 787 and 795

Nucleotide ^a		Mean CAT activity ^b	% Mutant 30 S in		Thermodynamics ^d	
787	795		30 S peak ^c	70 S peak ^c	ΔG_{37}° (kcal/mol)	T_m (°C)
A	<u>C</u>	100	46.1 ± 0.8	41.7 ± 3.3	-3.25	61.8
A	<u>A</u>	83.8 ± 2.5	n.d.	n.d.	-2.90	61.3
C	<u>C</u>	80.5 ± 0.5	n.d.	n.d.	-2.84	60.7
<u>C</u>	<u>U</u>	74.1 ± 3.4	n.d.	n.d.	n.d.	n.d.
A	<u>U</u>	72.1 ± 4.5	74.3 ± 0.5	14.3 ± 1.0	-5.62	75.3
<u>U</u>	<u>U</u>	72.0 ± 2.4	n.d.	n.d.	n.d.	n.d.
<u>G</u>	<u>U</u>	70.5 ± 1.8	56.1 ± 1.4	14.2 ± 0.6	-4.96	68.1
<u>U</u>	C	65.5 ± 2.1	n.d.	n.d.	-2.88	60.6
<u>C</u>	<u>A</u>	53.4 ± 1.0	n.d.	n.d.	n.d.	n.d.
<u>G</u>	<u>G</u>	52.9 ± 0.4	n.d.	n.d.	-3.70	64.9
<u>G</u>	<u>A</u>	46.0 ± 1.4	n.d.	n.d.	n.d.	n.d.
A	<u>G</u>	37.5 ± 0.5	n.d.	n.d.	-3.19	63.5
U	<u>A</u>	36.7 ± 0.4	70.8 ± 7.4	10.1 ± 0.4	-5.82	74.3
<u>U</u>	<u>G</u>	13.5 ± 3.3	57.7 ± 12.1	5.5 ± 3.4	-5.15	69.4
<u>G</u>	C	5.5 ± 1.8	58.3 ± 8.2	5.1 ± 1.3	-7.61	83.4
<u>C</u>	<u>G</u>	1.2 ± 0.1	n.d.	n.d.	n.d.	n.d.

Mutations are underlined. n.d., not determined.

^a Site-directed mutations were constructed using PCR as described for the random mutants (Figure 1) except that the mutagenic primers contained substitutions corresponding only to positions 787 and 795.

^b To determine ribosome function, each strain was grown and assayed for CAT activity at least twice. The data were averaged and are presented as percentages of the unmutated control, pRNA122 ± the standard error of the mean.

^c The ratio of plasmid to chromosome-derived rRNA in 30 S and 70 S ribosomes was determined by primer extension (Triman *et al.*, 1989). Cultures were grown and assayed at least twice and the mean values are presented as a percentage of the total 30 S in each peak ± the standard error of the mean.

^d Thermodynamic parameters are for the higher-temperature transition of model oligonucleotides (Figure 1) and are the average of results for four or five different oligomer concentrations. Standard errors for the ΔG_{37}° are ± 5% (1 kcal = 4184 J). Errors in T_m are estimated as ± 1 deg.C. All solutions were at pH 7.

function may be due to the inability of mutant 30 S and 50 S subunits to associate. Another explanation for this observation is that the mutations may directly affect a stage of the protein synthesis process prior to subunit association, such as initiation, which prevents subsequent steps from occurring. We have previously identified other mutations in the 16 S rRNA for which this appears to be the case (Cunningham *et al.*, 1993).

Thermodynamic analysis

The genetic data above indicate that ribosome function is strongly affected by structural interactions among nucleotides at the base of the loop. Base-pairs and mismatches are known to make different thermodynamic contributions to helix stability (SantaLucia *et al.*, 1991; Serra *et al.*, 1993). To examine the relationship between mismatch thermodynamics and ribosome function, we measured the stability of several model 790 loop hairpins (Figure 1(a)) containing substitutions corresponding to positions 787 and 795 (Table 3). The thermodynamic data show that loss of function correlated only weakly with stability of the nucleotide pair ($r^2 = 0.44$); however, notable exceptions exist. Thus, A·U and U·A form structures with very similar stabilities in model hairpins (see below) but are functionally very different (Table 3). Other pairs with similar stabilities but different levels of function include G·U and U·G or A·C and A·G. Thus, in addition to stability, structural and dynamic properties of the 787-795 pair appear to play a significant role in 790-loop function, perhaps through interaction with other molecules. Chemical protection studies also support a model in which the 790 loop undergoes conformational rearrangement during translation (Moazed & Noller, 1986). These investigators found that A794 and C795 were specifically protected from chemical modification by P-site bound tRNA in 30 S and 70 S ribosomes but were exposed in the absence of tRNA.

To investigate the physical basis for the sequence constraints identified in our selected mutants, we examined the structure and stability of model 790-loop RNA oligonucleotide hairpins (Figure 1(a)). Of our 78 selected mutants, 50 have the potential to form either A·C or G·U mismatches at positions 787, 795 (Table 1). Since protonated A·C (A⁺·C) and G·U are known to be isomorphous (Brown *et al.*, 1990; Hunter *et al.*, 1986), we measured the melting profile of the wild-type 790 sequence at pH 7 and at pH 5.3 (Figure 3). Both curves are biphasic with transitions at 20 to 30°C and 60 to 70°C. The higher melting transition is oligonucleotide concentration independent, indicating unimolecular unfolding of the hairpin. The lower transition, however, is concentration-dependent, suggesting that at low temperatures a bimolecular complex is formed such as an internal loop or that two hairpins are "kissing". Control experiments using an oligonucleotide containing the *E. coli* stem

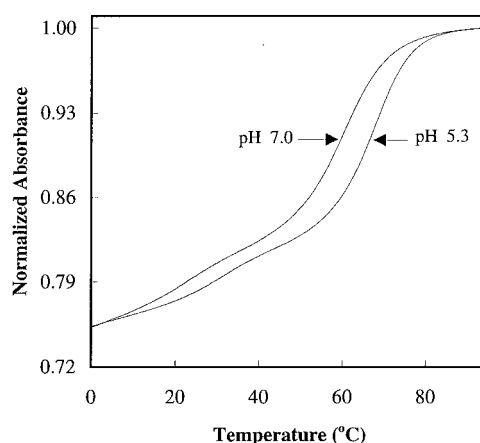


Figure 3. Normalized UV melting curves for rGGCGAUUAGAUACCGCC (underlined residues are in the loop) at pH 7 ($C_T = 1.5 \times 10^{-4}$ M) and pH 5.3 ($C_T = 1.0 \times 10^{-4}$ M).

sequence showed a decreased T_m for the bimolecular complex ($T_m \sim 10^\circ\text{C}$ at 10^{-4} M). Since the position of the T_m for the bimolecular complex is dependent on the stem sequence, this indicates that kissing hairpins are unlikely. The data show that the upper transition for A⁺·C at pH 5.3 is 1.6 kcal/mol ($\Delta T_m = 7^\circ\text{C}$) more stable than for A·C at pH 7. Thermodynamic measurements of mutations at positions 787 and 795 for which protonation is not necessary (G·U, G·C, A·U, U·A, U·G), showed no pH-dependence in either the upper transition or the lower transition (not shown).

NMR structural analysis

Next, we examined the imino proton region of the NMR spectrum (Figure 4(a)) to identify other hydrogen bonding and stacking interactions within the loop. The NMR spectrum of the wild-type sequence shows four imino resonances from the four base-pairs in the stem and one additional resonance from the loop at 14.15 ppm. Irradiation of the resonance at 14.15 ppm results in a strong nuclear Overhauser effect (NOE) to a resonance at 7.8 ppm (Figure 4(b)). These data and the NOE data presented below for the 787G and 795U mutant, indicate the presence of a Watson-Crick base-pair between positions 788U and 794A that is stacked on the weak pair formed between positions 787 and 795. These results suggest that the nucleotide covariations observed in our genetic studies among positions 787, 788, 794 and 795 are due to hydrogen bonding and stacking within the loop.

In our site-directed mutants, the G787-U795 double mutant produced ribosomes that were highly functional (Table 3). Guanine and uracil have imino protons that are convenient NMR spectroscopic markers. We therefore examined

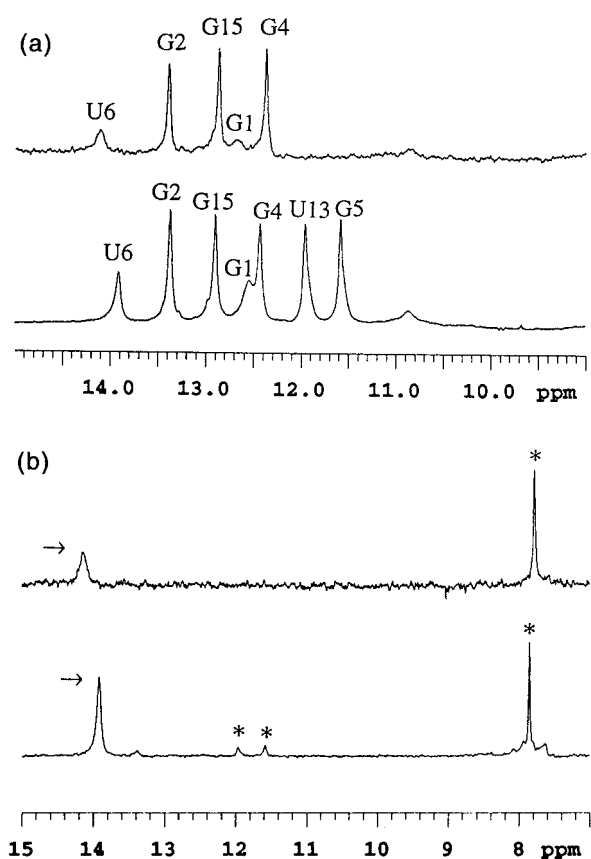


Figure 4. (a) The 1D NMR spectra of model 790 loop sequences dissolved in 90% H₂O, 10% ²H₂O. Top, 0.5 mM rGGCGAUUAGAUACCGCC in 50 mM NaCl, 10 mM sodium phosphate, 0.2 mM EDTA, pH 7, at 10°C. Broad resonances from 10 to 11.5 ppm are from the loop uridine and guanosine imino protons. Bottom, 2.3 mM rGGCGGUUAGAUUCGCC in 50 mM NaCl, 20 mM sodium phosphate, 0.2 mM EDTA, pH 7, at 10°C. Nucleotide assignments are indicated above each resonance (residues are numbered consecutively from G1 to C17). The integration and linewidth of the resonances in the wild-type and GU sequences indicate that resonances at 14.15 and 13.9 ppm are from the hairpin not the duplex form of the oligonucleotide (not shown). (b) Top, 1D-NOE difference spectrum for rGGCGAUUAGAUACCGCC with irradiation at 14.15 ppm (U6-imino). Note the strong NOE at 7.8 ppm (A12-H2). Bottom, 1D-NOE difference spectrum for rGGCGGUUAGAUUCGCC with irradiation at 13.9 ppm (U6-imino). Note the strong NOE at 7.8 ppm (A12-H2) and weak NOEs to 11.5 ppm (G5-imino) and 11.9 ppm (U13-imino). The irradiated resonances are indicated by arrows and NOEs by asterisks (*). The peak at 13.4 ppm is a spill-over artifact and does not appear in spectra acquired at lower saturation power.

the NMR spectroscopy of a mutant hairpin corresponding to the G787, U795 mutant and looked for the presence of NOEs involving the G787 and U795 imino protons. The G·U sequence shows all of the same features as the wild-type sequence and shows the expected resonances from the G·U mismatch. Assignments were obtained with-

out ambiguity by 1D-NOE difference spectroscopy and 2D-NOESY in H₂O and ²H₂O (not shown). For rGGCGGUUAGAUUCGCC, the G5 and U13 imino proton resonances at 11.5 and 11.9 ppm were distinguished by the chemical shift of their attached ¹⁵N at 144.2 ppm and 158.0 ppm, respectively, by natural abundance ¹H-¹⁵N gradient-HMQC (Szewczak *et al.*, 1993). The strong NOE observed from the G5 imino to the U13 imino proton indicates formation of a wobble pair (He *et al.*, 1991). Irradiation of the resonance at 13.9 ppm shows a strong NOE to the resonance at 7.8 ppm corresponding to the NOE from resonances at 14.15 ppm and 7.8 ppm in the wild-type sequence (Figure 4(b)). The similarity of the NMR data for G·U and A·C sequences indicates that in addition to isomorphous pairing of A787·C795 and G787·U795, the structures of both loops are isomorphous as well. This finding is consistent with our *in vivo* data, which show that ribosomes containing G787 and U795 are functional in both the randomized and site-directed mutants. The resonance at 13.9 ppm also shows weak NOEs to the G787 and U795 imino protons (Figure 4(b)). Based on these data we assign the 13.9 ppm resonance to U788. Natural abundance ¹H-¹³C-HMQC and NOESY of the G·U mutant in ²H₂O solution (not shown) indicate that the resonance at 7.8 ppm is the A794-H2 (the attached C2 chemical shift is 154.9 ppm: Varani & Tinoco, 1991). In addition, the H₂O-NOESY spectrum shows weak NOEs from both G787 and U795 imino protons to A794-H2 (not shown). These data indicate the formation of a Watson-Crick pair between U788 and A794 that is stacked on the 787-795 pair.

Conclusions

By simultaneously mutating all of the nucleotides in the 790 loop and selecting functional alternative sequences, we have identified four nucleotides whose role is primarily structural and two invariant nucleotides that may play a direct role in ribosome function. Since seven of the nine loop nucleotides showed considerable variation, it is unlikely that subunit association involves base-pairing between the 790 loop and the large subunit rRNA (Herr *et al.*, 1979). Our initial selection allowed identification of nucleotide preferences and covariations within the loop and revealed that nucleotides at positions 787 and 795 strongly affected ribosome function indirectly by affecting the structure of the loop. Site-directed mutations at positions 787 to 795 affected the ability of the mutant 30 S subunits to associate with 50 S subunits to form 70 S ribosomes. We also employed thermodynamic and NMR methods to determine the physical basis of our genetic data. The covariations observed among nucleotides at the base of the loop (788, 789, 794 and 795) were confirmed both

by site-directed mutagenesis and by physical methods.

The system described here allows facile elucidation of the relationship between the structure and function of ribosomal RNA *in vivo*. This approach complements phylogenetic analyses of rRNA structure by allowing analysis of highly conserved sequences through "instant evolution". This system may also be applied to the identification of inter- and intramolecular interactions by direct selection of second-site mutations that complement non-functional primary mutations. In addition, modification of the system should allow direct identification of elements of ribosomal RNA involved in each of the partial reactions of protein synthesis. These studies will lead to an improved understanding of the role of ribosomal RNA in protein synthesis and much needed information regarding the relationship of RNA sequence to RNA structure and function in biological systems

Materials and Methods

Reagents

Restriction enzymes, ligase, AMV reverse transcriptase and calf intestine alkaline phosphatase were from New England Biolabs and from Gibco-BRL. Sequenase modified DNA polymerase, nucleotides and sequencing buffers were from USB/Amersham. Oligonucleotides were synthesized on-site using a Beckman Oligo 1000 DNA synthesizer. Amplitaq DNA polymerase and PCR reagents were from Perkin-Elmer-Cetus. [³H]Chloramphenicol (30.1 Ci/mmol) was from Amersham and [α -³⁵S]dATP (1000 Ci/mmol) was from New England Nuclear. Other chemicals were from Sigma.

pRNA122

Construction of pRNA122 will be described elsewhere. The key features of this construct are: (1) it contains a copy of the *rrnB* operon from pKK3535 (Brosius *et al.*, 1981) under transcriptional regulation of the *lacUV5* promoter; (2) it contains a copy of the lactose repressor allele *lacI^q* (Calos, 1978); (3) the chloramphenicol acetyltransferase gene (*cam*) is present and transcribed constitutively from a mutant tryptophan promoter, *trp^c* (de Boer *et al.*, 1983; Hui *et al.*, 1987); (4) the RBS of the CAT message has been changed from the wild-type, 5'-GGAGG to 5'-AUCCC, and the MBS of the 16 S rRNA gene has been changed to 5'-GGGAU; (5) the β -lactamase gene is present to allow maintenance of plasmids in the host strain.

Bacterial strains and media

Plasmids were maintained and expressed in *E. coli* DH5 (*supE44*, *hsdR17*, *recA1*, *endA1*, *gyrA96*, *thi-1*; Hanahan, 1983). Cultures were grown in LB medium (Luria & Burrous, 1957) or LB medium containing 100 μ g/ml ampicillin (LB-Ap100). To induce synthesis of plasmid-derived rRNA from the *lacUV5* promoter, IPTG was added to a final concentration of 1 mM at the times indicated in each experiment. Strains were transformed by electroporation (Dower *et al.*, 1988) using a Gibco-BRL Cell Porator. Unless otherwise indicated, transformants were grown in SOC medium (Hanahan, 1983) for

one hour prior to plating on selective medium to allow expression of plasmid-derived genes.

Chloramphenicol acetyltransferase assays

CAT activity was determined essentially as described (Nielsen *et al.*, 1989). Cultures for CAT assays were grown in LB-Ap100. Briefly, 0.5 ml aliquots of mid-log cultures (unless otherwise indicated) were added to an equal volume of 500 mM Tris-HCl (pH8) and lysed using 0.01% (w/v) SDS and chloroform (Miller, 1992). The resulting lysate was either used directly or diluted in assay buffer prior to use. Assay mixtures contained cell extract (5 μ l or 10 μ l), 250 mM Tris (pH 8), 214 μ M butyryl-coenzyme A (Bu-CoA), and 40 μ M [³H]chloramphenicol in a 125 μ l volume. Two concentrations of lysate were assayed for one hour at 37°C to ensure that the signal was proportional to protein concentrations. The product, butyryl-[³H]chloramphenicol was extracted into 2,6,10,14-tetramethylpentadecane:xylene (2:1) and measured directly in a Beckman LS-3801 liquid scintillation counter. Blanks were prepared exactly as described above, except that uninoculated LB medium was used instead of culture.

Minimum inhibitory concentration determination

MICs were determined by standard methods in microtiter plates or on solid medium. Overnight cultures grown in LB-Ap100 were diluted and induced in the same medium containing 1 mM IPTG for three hours. Approximately 10⁴ induced cells were then added to wells (or spotted onto solid medium) containing LB-Ap100 + IPTG (1 mM) and chloramphenicol at increasing concentrations. Cultures were grown for 24 hours and the lowest concentration of chloramphenicol that completely inhibited growth was designated as the MIC.

Random mutagenesis and selection

Random mutagenesis of the 790 loop was performed essentially by the method of Higuchi (1989) using PCR and cloned in pRNA122 using the unique *Bgl*III and *Dra*III restriction sites (Figure 2). For each set of mutations, four primers were used: two "outside" primers and two "inside" primers. The two outside primers were designed to anneal to either side of the *Bgl*III and *Dra*III restriction sites in pRNA122 (Figure 2). These primers were 16 S-*Dra*III, 5'-GACAATCTGTGTGAGCACTA-3' and 16 S-535, 5'-TGCCAGCAGCCGCGTAATACG-GAGGGTGCAAGCGT-3'. The inside primers were 16 S-786R, 5'-CCTGTTTGCTCCCCACGCTTTCGCACCT-GAGCG-3' and 16 S-ASS-3, 5'-CTCAGGTGCGAAAGCG-TGGGGAGCAAACAGNNNNNNNNNCCTGGTA-GTCCACGCC GTAA-3' (N = A, T, C and G). Thus, 4⁹ = 262,144 possible combinations were created, with the exception of 320 sequences that were eliminated because they formed either *Bgl*III or *Dra*III recognition sites (256 *Bgl*III sites and 64 *Dra*III sites).

Transformants were incubated in SOC medium containing 1 mM IPTG for four hours to induce rRNA synthesis and then plated on LB agar containing 100 μ g/ml chloramphenicol. A total of 2 \times 10⁶ transformants were plated yielding approximately 2000 chloramphenicol-resistant survivors. Next, 736 of these survivors were randomly chosen and assayed to determine the MIC of chloramphenicol necessary to completely inhibit growth in cells expressing mutant ribosomes. From this pool,

182 transformants with MICs greater than 100 µg/ml were randomly selected and sequenced.

Site-directed mutation of positions 787 and 795

Mutations at positions 787 and 795 were constructed as described above for the random mutants, except that the inside primers were 16 S-786R (see above) and 16 S-ASS-4, 5'-CTCAGGTGCGAAAGCGTGGGGAGCAAA-CAGGNTTAGATANCCCTGGTAGTCCACGCCGTAA-3' (N = A, T, C and G). Transformants were selected on LB-Ap100 agar plates and grouped according to their MICs for chloramphenicol. Representatives from each group were then sequenced to identify the mutations.

Primer extension

To determine the ratio of plasmid to chromosome-derived rRNA, 30 S and 70 S ribosomes were isolated from 200 ml of induced, plasmid containing cells by the method of Powers & Noller (1991). The purified RNA was then used in primer extension experiments (Triman *et al.*, 1989). End-labeled primers complementary to sequences 3' to the 788 and 795 mutation sites were annealed to rRNA from induced cells and extended through the mutation site using AMV reverse transcriptase. The primers used were: 16 S-806R, 5'-GGACTACCAGGGTATCT-3'; 16 S-814R, 5'-TACGGCGTGGACTACCA-3'. For wild-type pRNA122 ribosomes, position 1192 in the 16 S RNA gene was changed from C to U and primers were constructed as described above (Triman *et al.*, 1989). This mutation has previously been shown not to affect subunit association (Sigmund *et al.*, 1988). The extension mixture contained a mixture of three deoxyribonucleotides and one dideoxyribonucleotide. The cDNAs were resolved by PAGE and the ratios of mutant to non-mutant ribosomes were determined by comparing the amount of radioactivity in each of the two bands.

Oligoribonucleotide synthesis

Oligoribonucleotides were synthesized on solid support with the phosphoramidite method (Capaldi & Reese, 1994) on a Cruachem PS 250 DNA/RNA synthesizer. Oligomers were removed from solid support and deprotected by treatment with ammonia and acid following the manufacturer's recommendations. The RNA was purified on a silica gel Si500F TLC plate (Baker) eluted for five hours with *n*-propanol/ammonia/water (55:35:10, by vol.). Bands were visualized with an ultraviolet lamp and the least mobile band was cut out and eluted three times with 1 ml of purified water. Oligomers were further purified with a Sep-pak C-18 cartridge (Waters) and desalted by continuous-flow dialysis (BRL). Purities were checked by analytical C-8 HPLC (Perceptive Biosystems) and were greater than 95%.

UV melting experiments

All solutions contained 50 mM NaCl, 20 mM sodium cacodylate, 0.2 mM EDTA at pH 7.0 or 5.3. Absorbance versus temperature curves were measured at 280 nm with a heating rate of 0.8 deg. C/minute on an AVIV 14DS UV-vis spectrophotometer as described (SantaLucia *et al.*, 1996). The curves were fit to a two-state model with sloping baselines using the non-linear least-squares program MELTWIN v3.0 (MacDowell & Turner, 1996).

NMR methods

Oligomers were dissolved in 50 mM NaCl, 10 mM sodium phosphate, and 0.5 mM Na₂EDTA, at pH 7. The solvent for imino proton studies was 10% ²H₂O, 90% H₂O. Spectra were acquired at 10°C on a Varian UNITY 500 MHz. NMR spectrometer using WATERGATE with "flip-back" solvent suppression (Lippens *et al.*, 1995; Piotto *et al.*, 1992). Spectra were recorded with the carrier placed at the solvent frequency and with high-power and low-power pulse-widths of 8.8 µs and 1700 µs, sweep-width of 12 kHz and gradient field strength of 10.0 G/cm and duration of 1 ms. 512 scans with 8192 points were collected for each spectrum. The data were multiplied by a 4.0 Hz line-broadening exponential function and Fourier transformed by a Silicon Graphics Indigo²Extreme computer with Varian VNMR software. No baseline correction or solvent subtraction was applied: 3-trimethylsilyl propionic-2,2,3,3-d⁴ acid was used as the internal standard for chemical shift reference. The 1D-NOE difference spectra were acquired as described above, but with selective decoupling of individual resonances during the one second recycle delay. Each resonance was decoupled with a power sufficient to saturate <80% of the signal intensity so that spill-over artifacts would be minimized. The spectra were acquired in an interleaved fashion in blocks of 16 scans to minimize subtraction errors due to long-term instrumental drift. In all, 4000 scans were collected for each FID.

Acknowledgments

We thank Robin Gutell for providing phylogenetic analyses and critical review of the manuscript. We thank Christine Chow, David Clark, Allen Nicholson, Jack Parker and Douglas H. Turner for critical review of the manuscript and helpful comments, and Hatim Allawi for technical assistance.

References

- Barta, A., Steiner, G., Brosius, J., Noller, H. F. & Kuechler, E. (1984). Identification of a site on 23S ribosomal RNA located at the peptidyl transferase center. *Proc. Natl Acad. Sci. USA*, **81**, 3607–3611.
- Brosius, J., Ullrich, A., Raker, M. A., Gray, A., Dull, T. J., Gutell, R. R. & Noller, H. F. (1981). Construction and fine mapping of recombinant plasmids containing the *rrnB* ribosomal RNA operon of *E. coli*. *Plasmid*, **6**, 112–118.
- Brow, D. A. & Noller, H. F. (1983). Protection of ribosomal RNA from kethoxal in polyribosomes. Implication of specific sites in ribosome function. *J. Mol. Biol.* **163**, 27–46.
- Brown, T., Leonard, G. A., Booth, E. D. & Kneale, G. (1990). Influence of pH on the conformation and stability of mismatch base-pairs in DNA. *J. Mol. Biol.* **212**, 437–40.
- Burns, D. K. & Crowl, R. M. (1987). *In vitro* mutagenesis of chloramphenicol acetyl transferase to investigate structure/function relationships. *Protein Struct. Fold. Des.* **2**, 375–384.
- Calos, M. P. (1978). DNA sequence for a low-level promoter of the *lac* repressor gene and 'up' promoter mutation. *Nature*, **274**, 762–769.

- Capaldi, D. & Reese, C. (1994). Use of the 1-(2-fluorophenyl)-4-methoxypiperidin-4-yl (Fmp) and related protecting groups in oligoribonucleotide synthesis: stability of internucleotide linkages to aqueous acid. *Nucl. Acids Res.* **22**, 2209–2216.
- Chapman, N. M. (1977). Protection of specific sites in 16S RNA from chemical modification by association of 30S and 50S ribosomes. *J. Mol. Biol.* **109**, 131–149.
- Cundliffe, E. (1986). Involvement of specific portions of ribosomal RNA in defined ribosomal functions: a study utilizing antibiotics. In *Structure, Function and Genetics of Ribosomes* (Hardesty, B. & Kramer, G., eds), pp. 486–604, Springer-Verlag, New York.
- Cunningham, P. R., Weitzman, C. J., Nègre, D., Sinning, J., Nurse, K. & Ofengand, J. (1992). G1401: A key-stone nucleotide at the decoding site of *Escherichia coli* 30S ribosomes. *Biochemistry*, **31**, 7629–7637.
- Cunningham, P. R., Nurse, K., Weitzmann, C. & Ofengand, J. (1993). Functional effects of base changes which further define the decoding center of *Escherichia coli* 16S ribosomal RNA: Mutation of C1404, G1405, C1496, G1497 and U1498. *Biochemistry*, **32**, 7172–7180.
- Dahlberg, A. E. (1989). The functional role of ribosomal RNA in protein synthesis. *Cell*, **57**, 525–529.
- de Boer, H. A., Comstock, L. J. & Vasser, M. (1983). The *tac* promoter: a functional hybrid derived from the *trp* and *lac* promoters. *Proc. Natl Acad. Sci. USA*, **80**, 21–25.
- de Stasio, E. A., Göringer, H. U., Tapprich, W. E. & Dahlberg, A. E. (1988). Probing ribosome function through mutagenesis of ribosomal RNA. In *Genetics of Translation* (Tuite, M. F., Picard, M. & Bolotin-Fukuhara, M., eds), pp. 17–42, Springer-Verlag, Berlin.
- Dower, W. J., Miller, J. F. & Ragsdale, C. W. (1988). High efficiency transformation of *E. coli* by high voltage electroporation. *Nucl. Acids Res.* **16**, 6127.
- Fourmy, D., Recht, M. I., Blanchard, S. C. & Puglisi, J. D. (1996). Structure of the A site of *Escherichia coli* 16S ribosomal RNA complexed with an aminoglycoside antibiotic. *Science*, **274**, 1367–1371.
- Gutell, R. R. (1994). Collection of small subunit (16S- and 16S-like) ribosomal RNA structures: 1994. *Nucl. Acids Res.* **22**(17), 3502–3507.
- Hanahan, D. (1983). Studies on transformation of *Escherichia coli* with plasmids. *J. Mol. Biol.* **166**, 557–580.
- He, L., Kierzek, R., SantaLucia, J., John, Walter, A. E. & Turner, D. H. (1991). Nearest-neighbor parameters for G·U mismatches. *Biochemistry*, **30**, 11124–11132.
- Herr, W., Chapman, N. & Noller, H. (1979). Mechanism of ribosomal subunit association: discrimination of specific sites in 16S RNA essential for association activity. *J. Mol. Biol.* **130**, 433–449.
- Higuchi, R. (1989). Using PCR to engineer DNA. In *PCR Technology* (Erlich, H. A., ed.), pp. 61–70, Stockton Press, New York.
- Huang, S., Wang, Y. X. & Draper, D. E. (1996). Structure of a hexanucleotide RNA hairpin loop conserved in ribosomal RNAs. *J. Mol. Biol.* **258**, 308–321.
- Hui, A. S. & de Boer, H. A. (1987). Specialized ribosome system: preferential translation of a single mRNA species by a subpopulation of mutated ribosomes in *Escherichia coli*. *Proc. Natl Acad. Sci. USA*, **84**, 4762–4766.
- Hui, A., Jhurani, P. & de Boer, H. A. (1987). Directing ribosomes to a single mRNA species: A method to study ribosomal RNA mutations and their effects on translation of a single messenger in *Escherichia coli*. *Methods Enzymol.* **153**, 432–452.
- Hunter, W. N., Brown, T., Anand, N. N. & Kennard, O. (1986). Structure of an adenine-cytosine base pair in DNA and its implications for mismatch repair. *Nature*, **320**, 552–555.
- Lata, R., Agrawal, R., Penczek, P., Grassucci, R., Zhu, J. & Frank, J. (1996). Three-dimensional reconstruction of the *Escherichia coli* 30S ribosomal subunit in ice. *J. Mol. Biol.* **262**, 43–52.
- Lee, K., Holland-Staley, C. A. & Cunningham, P. R. (1996). Genetic analysis of the Shine-Dalgarno interaction: selection of alternative functional mRNA-rRNA combinations. *RNA*, **2**, 1270–1285.
- Lippens, G., Dhalluin, C. & Wieruszski, J.-M. (1995). Use of a water flip-back pulse in the homonuclear NOESY experiment. *J. Biomol. NMR*, **5**, 327–331.
- Lodmell, J. S., Gutell, R. R. & Dahlberg, A. E. (1995). Genetic and comparative analyses reveal an alternative secondary structure in the region of nt 912 of *Escherichia coli* 16S rRNA. *Proc. Natl Acad. Sci. USA*, **92**, 10555–10559.
- Lu, M. & Draper, D. E. (1995). On the role of rRNA tertiary structure in recognition of ribosomal protein L11 and thiostrepton. *Nucl. Acids Res.* **23**, 3426–3433.
- Luria, S. E. & Burrous, J. W. (1957). Hybridization between *Escherichia coli* and *Shigella*. *J. Bacteriol.* **74**, 461–476.
- MacDowell, J. A. & Turner, D. H. (1996). Investigation of the structural basis for thermodynamic stabilities of tandem GU mismatches: solution structure of (rGAGGUCUC)₂ by two-dimensional NMR and simulated annealing. *Biochemistry*, **35**, 14077–14089.
- Maidak, B. L., Olsen, G. J., Larsen, N., Overbeek, R., McCaughey, M. J. & Woese, C. R. (1996). The ribosomal database project (RDP). *Nucl. Acids Res.* **24**, 82–85.
- Miller, J. H. (1992). Procedures for working with *lac*. In *A Short Course in Bacterial Genetics* (Miller, J. H., ed.), pp. 71–80, Cold Spring Harbor Laboratory Press, Cold Spring Harbor, NY.
- Moazed, D. & Noller, H. F. (1986). Transfer RNA shields specific nucleotides in 16S ribosomal RNA from attack by chemical probes. *Cell*, **47**, 985–994.
- Moazed, D., Van Stolk, B. J., Douthwaite, S. & Noller, H. F. (1986). Interconversion of active and inactive 30S ribosomal subunits is accompanied by a conformational change in the decoding region of 16S rRNA. *J. Mol. Biol.* **191**, 483–493.
- Moazed, D., Samaha, R. R., Gualerzi, C. & Noller, H. F. (1995). Specific protection of 16S rRNA by translational initiation factors. *J. Mol. Biol.* **248**, 207–210.
- Moine, H. & Dahlberg, A. E. (1994). Mutations in helix 34 of *Escherichia coli* 16S ribosomal RNA have multiple effects on ribosome function and synthesis. *J. Mol. Biol.* **243**, 402–412.
- Muralikrishna, P. & Wickstrom, E. (1989). *Escherichia coli* initiation factor 3 protein binding to 30S ribosomal subunits alters the accessibility of nucleotides within the conserved central region of 16S rRNA. *Biochemistry*, **28**, 7505–7510.
- Nielsen, D. A., Chang, T. & Shapiro, D. J. (1989). A highly sensitive, mixed-phase assay for chloramphenicol acetyltransferase activity in transfected cells. *Anal. Biochem.* **179**, 19–23.
- Noller, H. F. (1991). Ribosomal RNA and translation. *Annu. Rev. Biochem.* **60**, 191–227.

- Noller, H. F., Hoffarth, V. & Zimniak, L. (1992). Unusual resistance of peptidyl transferase to protein extraction procedures. *Science*, **256**, 1416–1419.
- Piotto, M., Saudek, V. & Sklenar, V. (1992). Gradient-tailored excitation for single-quantum NMR spectroscopy of aqueous solutions. *J. Biomol. NMR*, **2**, 661–665.
- Powers, T. & Noller, H. F. (1991). A functional pseudoknot in 16S ribosomal RNA. *EMBO J.* **10**, 2203–2214.
- Ryan, P. C. & Draper, D. E. (1991). Detection of a key tertiary interaction in the highly conserved GTPase center of large subunit ribosomal RNA. *Proc. Natl Acad. Sci. USA*, **88**, 6308–6312.
- SantaLucia, J., Jr, Kierzek, R. & Turner, D. H. (1991). Stabilities of consecutive A·C, C·G, U·C, and U·U mismatches in RNA internal loops: evidence for stable hydrogen-bonded U·U and C·C+ pairs. *Biochemistry*, **30**, 8242–8251.
- SantaLucia, J., Allawi, H. T. & Seneviratne, P. A. (1996). Improved nearest-neighbor parameters for predicting DNA duplex stability. *Biochemistry*, **35**, 3555–3562.
- Santer, M. & Shane, S. (1977). Area of 16 S ribonucleic acid at or near the interface between the 30 S and 50 S ribosomes of *Escherichia coli*. *J. Bacteriol.* **130**, 900–910.
- Serra, M. J., Lyttle, M. H., Axenson, T. J., Schadt, C. A. & Turner, D. H. (1993). RNA hairpin loop stability depends on closing base pair. *Nucl. Acids Res.* **21**, 3845–3849.
- Shine, J. & Dalgarno, L. (1974). The 3'-terminal sequence of *E. coli* 16 S ribosomal RNA: complementarity to nonsense triplets and ribosome binding sites. *Proc. Natl Acad. Sci. USA*, **71**, 1342–1346.
- Sigmund, C. D., Ettayebi, M., Borden, A. & Morgan, E. A. (1988). Antibiotic resistance mutations in ribosomal RNA genes of *Escherichia coli*. *Methods Enzymol.* **164**, 673–689.
- Szewczak, A. A. & Moore, P. B. (1995). The sarcin/ricin loop, a modular RNA. *J. Mol. Biol.* **247**, 81–98.
- Szewczak, A. A., Kellogg, G. W. & Moore, P. B. (1993). Assignment of NH resonances in nucleic acids using natural abundance ¹⁵N-¹H correlation spectroscopy with spin-echo and gradient pulses. *FEBS Letters*, **327**, 261–264.
- Tapprich, W. & Hill, W. (1986). Involvement of bases 787-795 of *Escherichia coli* 16 S ribosomal RNA in ribosomal subunit association. *Proc. Natl Acad. Sci. USA*, **83**, 556–560.
- Tapprich, W. E., Goss, D. J. & Dahlberg, A. E. (1989). Mutation at position 791 in *Escherichia coli* 16 S ribosomal RNA affects processes involved in the initiation of protein synthesis. *Proc. Natl Acad. Sci. USA*, **86**, 4927–4931.
- Triman, K., Becker, E., Dammel, C., Katz, J., Mori, H., Douthwaite, S., Yapijakis, C., Yoast, S. & Noller, H. F. (1989). Isolation of temperature-sensitive mutants of 16 S rRNA in *E. coli*. *J. Mol. Biol.* **209**, 643–653.
- Varani, G. & Tinoco, I., Jr (1991). Carbon assignments and heteronuclear coupling constants for an RNA oligonucleotide from natural abundance ¹³C-¹H correlated experiments. *J. Am. Chem. Soc.* **113**, 9349–9354.
- Zimmermann, R. A. & Dahlberg, A. E., editors (1996). *Ribosomal RNA*, CRC Press, Boca Raton, FL.

Edited by D. E. Draper

(Received 10 February 1997; received in revised form 8 April 1997; accepted 9 April 1997)